Journal of Sound and Vibration 327 (2009) 604–622

Contents lists available at ScienceDirect

Journal of Sound and Vibration

journal homepage: www.elsevier.com/locate/jsvi

Model based fault diagnosis of a rotor–bearing system for misalignment and unbalance under steady-state condition

Arun Kr. Jalan, A.R. Mohanty *

Department of Mechanical Engineering, Indian Institute of Technology, Kharagpur 721 302, West Bengal, India

ARTICLE INFO

Article history:
Received 6 August 2008
Received in revised form
6 July 2009
Accepted 17 July 2009
Handling Editor: L.G. Tham
Available online 6 August 2009

ABSTRACT

Vibration monitoring is one of the primary techniques of condition monitoring of rotating machines. Shaft misalignment and rotor unbalance are the main sources of vibration in rotating machines. In this study a model based technique for fault diagnosis of rotor–bearing system is described. Using the residual generation technique, residual vibrations are generated from experimental results for the rotor bearing system subject to misalignment and unbalance, and then the residual forces due to presence of faults are calculated. These residual forces are compared with the equivalent theoretical forces due to faults. The fault condition and location of faults are successfully detected by this model based technique.

1. Introduction

Rotating machines are important assets in most of the industries. The rotor–bearing system of modern rotating machinery is complex which needs accurate and reliable prediction of its dynamic characteristics. Shaft misalignment and disk unbalance are the two main sources of rotating machinery vibration. The vibration due to such sources affects critical parts of the system such as bearings, gears, motor, seals, couplings etc.

Shaft misalignment is a condition in which the shafts of the driving and driven machines are eccentric because of improper machine assembly. "Perfect alignment" of the driving and driven shafts cannot be achieved in practical applications. Even if perfect alignment is achieved initially, it would not be possible to maintain it during operation of the machine due to various factors such as thermal distortion of housing supports of the bearings, differential thermal growth of machine parts, piping forces due to variation in pressure and temperature, movement of foundation etc. Thus, a misalignment condition is virtually always present in machine-trains. Usually flexible couplings are used to accommodate the existing misalignment between shafts and to transmit rotary power without torsional slip. Modeling of flexible coupling as discussed by Kramer [1] is utilized in this study.

In defiance of its importance, the study of shaft misalignment is still inadequate. Few researchers have given attention to shaft misalignment due to complexity in modeling. In an attempt to know the dynamic behavior for shaft misalignment of a rotor–coupling–bearing system, Xu and Marangoni [2] developed a theoretical model for angular misalignment, but in this model bearing damping and gyroscopic effects in the system are not considered and bearings are considered as rigid supports.

Misalignment in rotating machinery causes reaction forces and moments to be generated in the coupling which leads to vibration in the system. The effect of these forces and moments on the system has been described by [3–5] to reveal their

* Corresponding author. Tel.: +91 3222 282944; fax: +91 3222 255303.
E-mail address: amohanty@mech.iitkgp.ernet.in (A.R. Mohanty).

0022-460X/$ - see front matter © 2009 Elsevier Ltd. All rights reserved.
doi:10.1016/j.jsv.2009.07.014

Nomenclature

c^b_{HH}, c^b_{HV}	bearing damping along horizontal direction about horizontal and vertical direction, respectively
c^b_{VH}, c^b_{VV}	bearing damping along vertical direction about horizontal and vertical direction, respectively
C^b	damping matrix of bearing
$FX1$, $FX2$	reaction forces
G^d	damping matrix of disk
G^e	damping matrix of shaft element
I	diametral inertia of element
I_D, I_P	disk diametral inertia and polar inertia
k^b_{HH}, k^b_{HV}	bearing stiffness along horizontal direction about horizontal and vertical direction, respectively
k^b_{VH}, k^b_{VV}	bearing stiffness along vertical direction about horizontal and vertical direction, respectively
K_a, K_b	axial and bending spring rate per degree per disk pack
K^b	stiffness matrix of bearing
K^e_B	bending stiffness matrix of shaft element
K^e_A	axial load stiffness matrix of shaft element
l	element length
m	element mass per unit length
$MX1$, $MX2$	reaction moments
M_d	mass of disk
M^d_T	translation mass matrix of disk
M^d_R	rotational mass matrix of disk
M^e_T	translation mass matrix of shaft element
M^e_R	rotational mass matrix of shaft element
q	generalized coordinates
r	radius of element
T_q	torque
$\Delta X1$, $\Delta Y1$	misalignment in X, Y direction at node 1
$\Delta X2$, $\Delta Y2$	misalignment in X, Y direction at node 2
$Z3$	center of articulation
θ	misalignment angle
θ_1	$\sin^{-1}(\Delta X1/Z3)$
θ_2	$\sin^{-1}(\Delta X2/Z3)$
ϕ_1	$\sin^{-1}(\Delta Y1/Z3)$
ϕ_2	$\sin^{-1}(\Delta Y2/Z3)$

influence on machine components such as bearings, shaft etc. Shaft misalignment has been represented in frequency domain as a series of harmonics of the shaft running speed [6] whereas investigators like Piotrowski [7], Xu and Marangoni [2], have furnished vibration identification charts which indicate that coupling misalignment produces a frequency which is twice of shaft speed frequency. This study showed that the vibration response due to coupling misalignment largely affect the even multiples (i.e. $2\times$, $4\times$, etc. components) of running speed.

Disk unbalance is a condition in which the center of mass of a rotating disk is not coincident with the center of rotation. Unbalance in a rotor system is unavoidable and it cannot be completely eliminated. In practice, balancing is done to balance the rotor system but due to some reasons, such as porosity in casting, non-uniform density of material, manufacturing tolerances, and gain or loss of material during operation, rotors can never be perfectly balanced. A fault model for unbalance has been developed by Platz and Markert [8] by considering equivalent loads at particular point due to unbalance.

The generalized equation of motion for a complete rotor–bearing system is derived using the finite element method given by Nelson and McVaugh [9]. The flexible coupling effect is included in the model to take misalignment into account. To achieve the effect of misalignment a periodic force is considered at coupling.

In the present study a model based fault diagnosis technique is developed for identifying the faults of a rotor–coupling–bearing system subject to misalignment and unbalance at a steady-state condition. This model based fault diagnosis technique is based on residual generation which is elaborately described by Isermann [10]. Sekhar [11] have presented a model based technique for the shaft crack identification by residual generation. However, a detailed review on different fault identification technique of cracked rotor system is presented by Sekhar [12]. In this study, model based residual generation technique is applied to identify misalignment and unbalance of a rotor system.

2. Model based fault identification method

For the improvement of reliability, safety and efficiency of technical processes, fault detection and fault diagnosis are being used as advanced supervision tools in present industries. The automated early detection and localization of faults in machines are of paramount importance. The conventional approaches is to monitor some important variables like pressure, temperature, vibration and generate alarms if certain limits are exceed but these approaches do not give a deeper insight and detect the internal faults at a rather late stage. By applying static and dynamic process models, common process input and output measurements, the inherent relationships and redundancies can be used to detect faults earlier and localize them better. This model based methods of fault detection are developed based on parameter estimation, parity equations or state observers.

The early contribution towards parity equation based fault diagnosis was made by Chow and Willsky [13] and then further developed by Gertler [14]. The main idea behind this approach is to check the consistency of the mathematical system equation by using an actual measurement. Frank and Keller [15] had given a concept of dedicated observer approach for detection and isolation of faults. According to this approach the outputs of the system are reconstruct with the

aid of the observers using estimation error. All these approaches lead to the concept of state estimation. Apart from these approaches there is an alternative method of fault diagnosis as parameter identification approach. A detailed description of this approach is given by Isermann [16] and Patton et al. [17].

The general procedure of model based fault detection and isolation can be roughly divided into generation of residuals [16] (i.e. functions that are emphasized by fault vector), diagnosis and isolation of faults. The fault detection methods generate residuals, parameter estimates or state estimates which are known as features. By comparison of the actual features with the normal features, changes in features are detected, known as residual generation which gives the analytical symptoms.

2.1. Residual generation

The residual generation problem can be stated by considering a dynamic system with a known nominal mathematical model. For a given actual input vector and measured output vector, the residual vector $\vec{r}$, that carries information about a particular fault, can be generated under the following conditions discussed by Frank [15]:

(a) The mode (time evolution) of the fault is unknown.
(b) The mathematical model of the nominal system is uncertain.
(c) The residual generation as to be performed in a specified time.
(d) There is system noise and measurement noise with unknown characteristics.

For the detectable and distinguishable fault, the system should satisfy the following condition:

(a) Knowledge of the normal behavior.
(b) Definitiveness of the faulty behavior.
(c) Existence of analytical redundancy relations.
(d) Availability of at least one observation reflecting the fault.
(e) Satisfactory reliability of redundant information.

2.2. Mathematical description

The vibrations represented by the vector $x_0(t)$ at N DOF of the healthy rotor system due to the operating load $F(t)$ during normal operation is described by the linear equation of motion

$$M\ddot{x}_0(t) + C\dot{x}_0(t) + Kx_0(t) = F(t) \tag{1}$$

where M, C and K are mass, damping, and stiffness matrices of any complex rotor system which includes the effect of bearings, foundations, gyroscopic effects etc.

The occurrence of a fault in the system changes its dynamic behavior. The extent of the change depends on the vector β, which describes the fault parameters such as type, location, magnitude etc. of the fault, for e.g. for misalignment: type of misalignment (angular or parallel), amount of misalignment. The fault-induced change in the vibrational behavior is represented by the additional loads acting on the healthy system:

$$M\ddot{x}(t) + C\dot{x}(t) + Kx(t) = F(t) + \Delta F(\beta, t) \tag{2}$$

The residual vibrations induced represent the difference of previously measured normal vibrations $x_0(t)$ of healthy system from currently measured vibrations $x(t)$ of faulty system. The residuals of vibration may thus be written as

$$\Delta x(t) = x(t) - x_0(t); \quad \Delta\dot{x}(t) = \dot{x}(t) - \dot{x}_0(t); \quad \Delta\ddot{x}(t) = \ddot{x}(t) - \ddot{x}_0(t) \tag{3}$$

Subtraction of the equations of motion for the healthy system (Eq. (1)) from that of faulty system (Eq. (2)), and using Eq. (3), the equation of motion for residual vibration can be represented as

$$M\Delta\ddot{x}(t) + C\Delta\dot{x}(t) + K\Delta x(t) = \Delta F(\beta, t) \tag{4}$$

The system matrices remain unchanged and the rotor model remains linear. Only the equivalent loads induce the change in the dynamic behavior of the healthy linear rotor model. To identify the fault parameters, the difference of the theoretical fault model and the measured equivalent loads will be minimized by some statistical algorithm like least square fitting.

To calculate the fault induced residual vibrations, there is a need of measured vibration data for both healthy and faulty rotor system at same operating and measurement conditions. Directly matching data is usually not available for generating residual vibrations. Hence some signal processing has to be carried out to achieve the same conditions. For example different rotor speeds are compensated by adjusting the time scale of the recorded normal vibrations to the time scale of currently measured vibrations. Phase shifts are avoided by recording a trigger signal during the measurement [8,18].

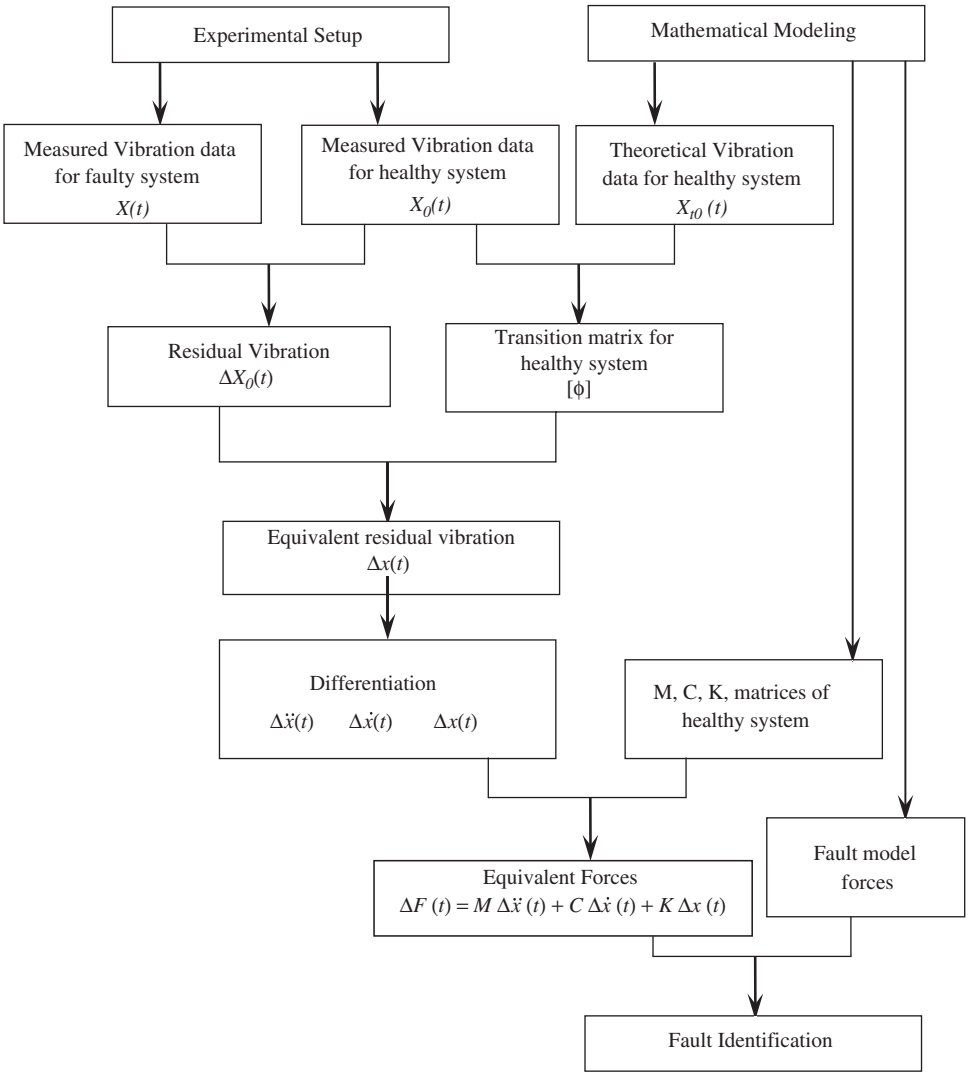

Fig. 1. Flow chart for fault identification.

2.3. Scheme of fault diagnosis

To identify the fault in any system a model based scheme is established with the help of residual generation. The flow chart of this scheme is shown in Fig. 1.

The pre-requisite for this kind of fault diagnosis is the measured vibration signal data for the healthy rotor system in the form of displacement which can be written as "$X_0(t)$". Now in order to find out the fault in the system, measured vibration signal data for the faulty system are stored in the form of displacement which can be written as "$X(t)$". The residual vibration is calculated from the measured vibration displacement data for both the healthy system and the faulty system at same operating conditions. The residual displacement is given by $\Delta X_0(t)$:

$$\Delta X_0(t) = X(t) - X_0(t) \tag{5}$$

Next a transition matrix is estimated to make a relationship between theoretical vibration response of the healthy system and measured vibration response of healthy system. This transition matrix $[\phi]$ is used to compute the equivalent residual vibration for the theoretical model:

$$[\phi] = X_0^{\mathrm{T}}(t) \cdot X_{t0}(t) \tag{6}$$

$$\Delta x(t) = [\phi] \cdot \Delta X_0(t) \tag{7}$$

where $X_{t0}(t)$ is the theoretical vibration response of the system and $\Delta x(t)$ the equivalent residual displacement for theoretical model.

At each position of the rotor system, displacements are measured and by residual generation displacement residuals are only calculated. But for fault diagnosis process there is a need of all three type of signal i.e. accelerations, velocities and displacements at each position. The equivalent residual velocities ($\Delta\dot{x}(t)$) and accelerations ($\Delta\ddot{x}(t)$) for theoretical model are obtained by differentiating the equivalent residual displacement signal.

To calculate the equivalent loads from the mathematical model of the rotor system there is a need of measured residual vibrations at all DOF of the model. But practically it is not possible to install the vibration sensors at all the locations. The number of measurement locations is much smaller than the number of model's DOF. To resolve this problem the residual vibrations of the non-measurable DOF have to be estimated from the measured residual vibrations. Therefore, the residual vibrations need to be reconstructed via modal expansion [11].

The equivalent forces characterizing the unknown faults are calculated by substituting the residual displacements, residual velocities and residual accelerations of the full vibrational state into Eq. (4):

$$\Delta F(t) = M\Delta\ddot{x}(t) + C\Delta\dot{x}(t) + K\Delta x(t) \tag{8}$$

Only simple matrix multiplications and additions have to be carried out on-line for calculating the equivalent loads from the measured vibration signals.

Now, for the proposed model based fault diagnosis method, each fault has to be representing by a mathematical model describing the relationship between the fault parameters and the equivalent forces. The fault-induced change of the rotor system is taken into account by equivalent loads which are acting on the healthy system model to generate a dynamic behavior identical to the measured faulty system. By comparing the results from the fault models and measured equivalent loads from Eq. (8), the type, amount and location of the fault can be estimated.

3. Modeling of rotor system

The rotor–coupling–bearing system is considered to be a set of interconnecting components comprising a rigid disk, shaft segments with distributed mass and elasticity, and bearings.

3.1. Rotor disk

The equation of motion of the rigid disk is developed using Lagrangian formulation by Nelson [9] with finite element method by considering four DOF, two translation motions H and V in horizontal and vertical direction, respectively, and two rotational motions B and r about horizontal and vertical axis, respectively, at each node. The Lagrangian equation of motion of the rigid disk with constant spin speed is given by

$$([M_T^d] + [M_R^d])\{\ddot{q}^d\} - \Omega[G^d]\{\dot{q}^d\} = \{Q^d\} \tag{9}$$

where

$$\{q\} = \begin{Bmatrix} H \\ V \\ B \\ r \end{Bmatrix}$$

The individual element matrices are provided in Appendix A. The forcing term on the right hand side of Eq. (9) includes unbalance mass, inter-connecting forces and other external effects on the disk.

3.2. Finite shaft element

A typical finite shaft element time dependent cross section displacements are functions of position(s) along the axis of the element. The equation of motion for the finite shaft element is derived using Lagrangian formulation by Nelson [9]. The Lagrangian equation of motion of the finite shaft element with constant spin speed is given by

$$([M_T^e + M_R^e])\{\ddot{q}^e\} - \Omega[G^e]\{\dot{q}^e\} + ([K_B^e + K_A^e])\{q^e\} = \{Q^e\} \tag{10}$$

The individual element matrices are provided in Appendix A. The forcing term on the right hand side of Eq. (10) includes unbalance mass, inter-connecting forces and other external effects on the shaft elements.

3.3. Bearings

Generally anti-friction bearings are used in high speed rotating machines due to their long life, excellent damping characteristics, light weight, high load carrying capacity and low cost. The equation of motion for a bearing is derived in a similar way as in Ref. [9]. The linear bearings in the present FEM notations are represented by governing equation

of the form

$$[C^b]\{\dot{q}^b\} + [K^b]\{q^b\} = \{Q^b\} \tag{11}$$

where

$$\{q^b\} = \begin{Bmatrix} H \\ V \end{Bmatrix}, \quad [K^b] = \begin{bmatrix} k^b_{HH} & k^b_{HV} \\ k^b_{VH} & k^b_{VV} \end{bmatrix}, \quad [C^b] = \begin{bmatrix} c^b_{HH} & c^b_{HV} \\ c^b_{VH} & c^b_{VV} \end{bmatrix}$$

and $\{Q^b\}$ is bearing external force vector.

3.4. Equation of motion

The assembled equation of motion of rotor system may be written as

$$[M]\{\ddot{q}\} + [C]\{\dot{q}\} + [K]\{q\} = \{Q\} \tag{12}$$

where the mass matrix $[M]$ includes the translational and rotary mass matrices of shaft elements and rigid disk and the matrix $[C]$ includes gyroscopic moments and bearing damping. The stiffness matrix $[K]$ includes stiffness of the shaft elements and bearing stiffness. The excitation matrix Q comprises weight of rigid disk, unbalance excitation force, bearing force, forces due to fault in rotor system and other external forces.

4. Fault modeling

4.1. Coupling misalignment

Vibration in rotating machinery is a major concern for modern industries where shaft misalignment in rotor–bearing system is a common and main source of vibration. Misalignment means that the components of the system are not coaxial due to their functions. Usually couplings are used to accommodate the existing misalignment between shafts. Although, coupling is inexpensive compared to the system, it is a critical part of any rotor system and a good deal of attention is needed. The separate shafts of a complete line-out can be connected together by either rigid or flexible couplings. For rigid couplings the connection is treated as two connected beam elements. Generally flexible coupling is used in rotating machinery because it allows some misalignment between the two adjacent shaft rotation axes. Modeling of flexible coupling as discussed by Kramer [1] is utilized in this study. The flexibility in the coupling can be modeled by assuming the coupling to be comprised of two shaft elements connected together by a frictionless joint. The stiffness matrix for the coupling is provided in Appendix A.

Misalignment in rotating machinery causes reaction forces and moments to be generated in the coupling. There are two basic types of shaft misalignment, parallel misalignment and angular misalignment, as shown in Fig. 2. Gibbons [3] has given the reaction forces and moments developed due to parallel misalignment. The reaction forces and moments due to angular misalignment are given by Sekhar [4] and Prabhakar et al. [5]. The reaction forces and moments which the coupling

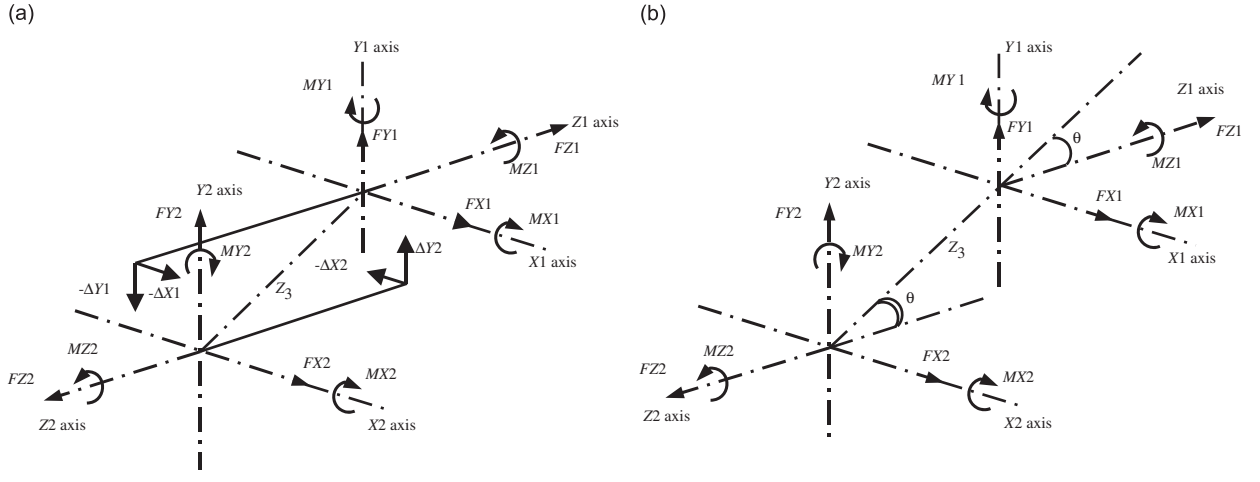

Fig. 2. Coupling coordinate system: (a) parallel misalignment and (b) angular misalignment.

exerts on the machine's shaft are as follows:

For parallel misalignment:

$$MX1 = Tq \sin\theta_1 + K_b\phi_1, \quad MX2 = Tq \sin\theta_2 - K_b\phi_2$$

$$MY1 = Tq \sin\phi_1 - K_b\theta_1, \quad MY2 = Tq \sin\phi_2 + K_b\theta_2$$

$$FX1 = (-MY1 - MY2)/Z3, \quad FX2 = -FX1$$

$$FY1 = (MX1 + MX2)/Z3, \quad FY2 = FY2 \tag{13}$$

For angular misalignment:

$$MX1 = 0.0, \quad MX2 = -K_b\theta, \quad MY1 = 0.0$$

$$MY2 = Tq \sin\theta, \quad MZ1 = Tq/\cos\theta, \quad MZ2 = -Tq$$

$$FX1 = (-MY1 - MY2)/Z3, \quad FX2 = -FX1$$

$$FY1 = (MX1 + MX2)/Z3, \quad FY2 = -FY2 \tag{14}$$

The above mentioned reaction forces and moments are the static load for a non-rotating rotor. For a rotating shaft they are acting as a periodic load with a function of half-sinusoidal having time period of π/Ω. For numerical analysis 1Ω and 2Ω components of the reaction forces are considered and they are incorporated into the excitation matrix in equation of motion at the corresponding DOF. The nodal force vectors due to coupling misalignment are given as

$$\{Q_c^1\} = \begin{Bmatrix} FX1 \sin\Omega t + FX1 \sin 2\Omega t \\ FY1 \cos\Omega t + FY1 \cos 2\Omega t \\ 0 \\ 0 \end{Bmatrix}, \quad \{Q_c^2\} = \begin{Bmatrix} FX2 \sin\Omega t + FX2 \sin 2\Omega t \\ FY2 \cos\Omega t + FY2 \cos 2\Omega t \\ 0 \\ 0 \end{Bmatrix} \tag{15}$$

where $\{Q_c^1\}$ and $\{Q_c^2\}$ are the nodal force vectors at the left and right side of the coupling.

4.2. Disk unbalance

In industrial rotor–bearing system rotor unbalance is a common and major source of vibration. Presence of unbalance changes the dynamic behavior of the system. This change is taken into account by equivalent loads acting on the healthy

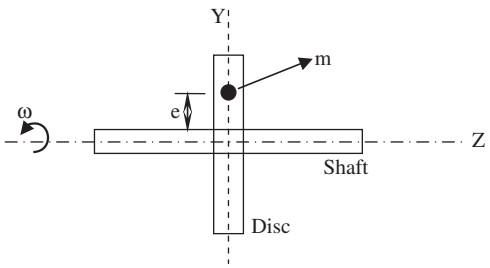

Fig. 3. Static disk unbalance.

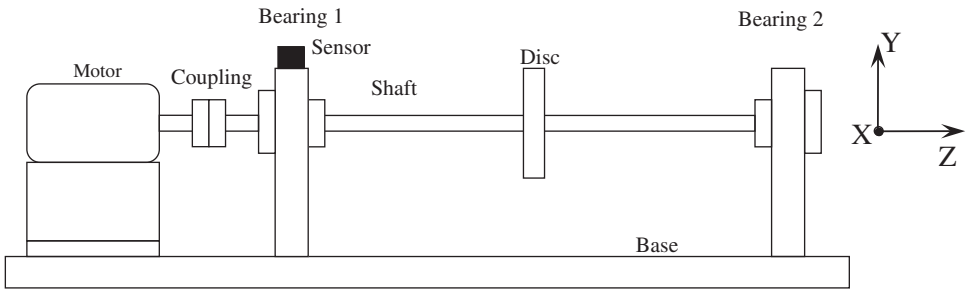

Fig. 4. Rotor–coupling–bearing test rig.

system model. Equivalent loads on the system generate a dynamic behavior identical to that of the real faulty system. The fault model for unbalance, developed by Platz [8] describes the effect of static and kinetic unbalances of the rotor system. The static unbalance is present in the system due to shift of mass center of mounted disk, resulting in an equivalent force.

The unbalance forces are effective in the lateral directions at the disk, in x–y plane, and are given by

$$F_x = me\omega^2 \cos \omega t, \quad F_y = me\omega^2 \sin \omega t \tag{16}$$

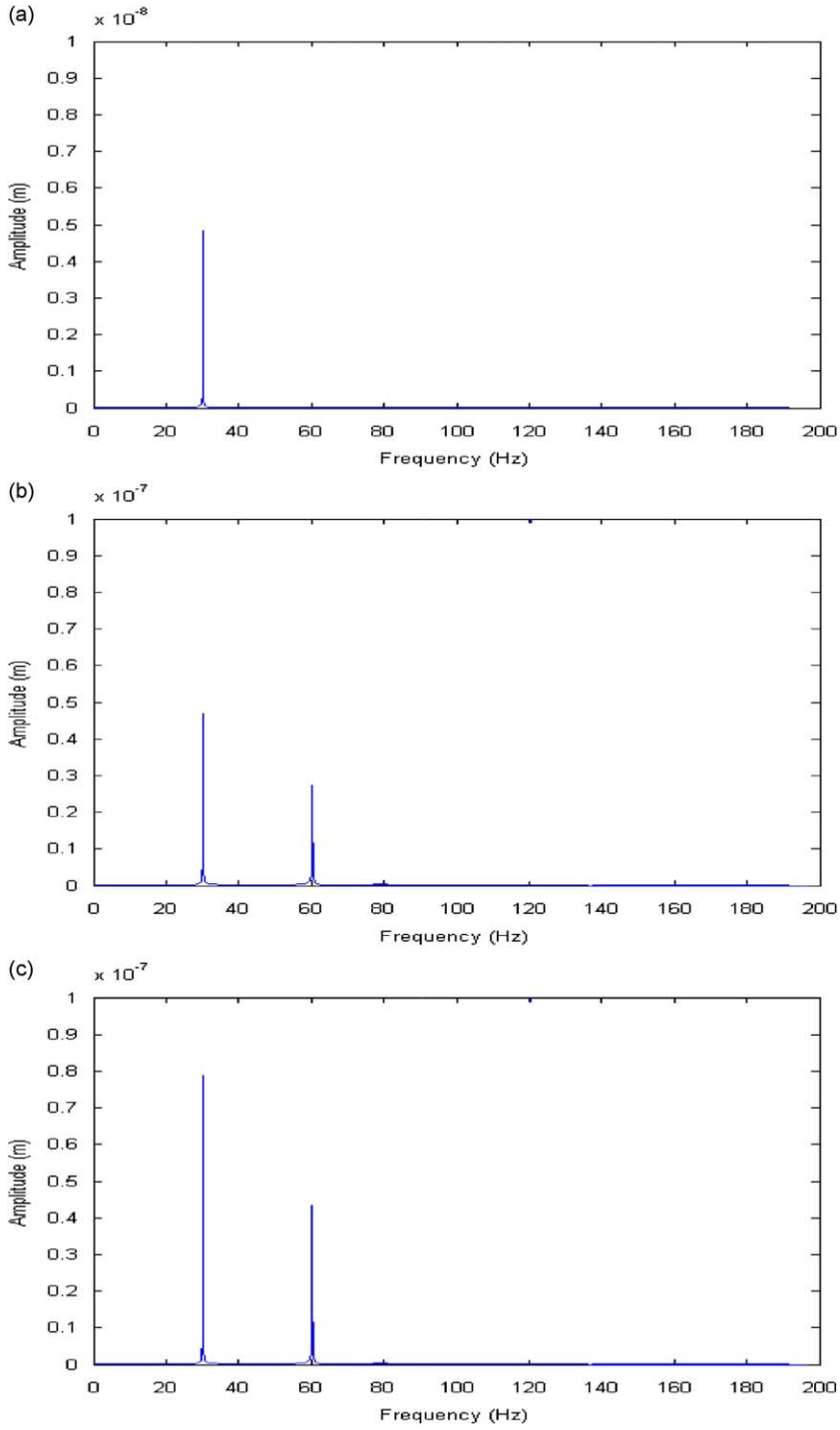

Fig. 5. Displacement spectra of a rotor–coupling–bearing system: (a) without misalignment; (b) with parallel misalignment and (c) with angular misalignment at bearing 1 location.

where m is the mass of unbalance in the disk located at distance "e" as shown in Fig. 3. ω is angular speed of rotor and t is time.

The excitation matrix Q of Eq. (12) can be written as

$$\{Q\} = \begin{bmatrix} 0 \\ \vdots \\ 0 \\ Q_d \\ 0 \\ \vdots \\ 0 \end{bmatrix} = \begin{bmatrix} 0 \\ \vdots \\ 0 \\ me\omega^2 \cos \omega t \\ me\omega^2 \sin \omega t \\ 0 \\ \vdots \\ 0 \end{bmatrix} \tag{17}$$

where $\{Q_d\}$ is excitation matrix for disk static unbalance.

5. Numerical simulation

A rotor–coupling–bearing system as shown in Fig. 4 has been considered for analysis. Modeling matrices (i.e. mass, stiffness and damping) required for shaft and disk can be calculated by their material properties and geometrical

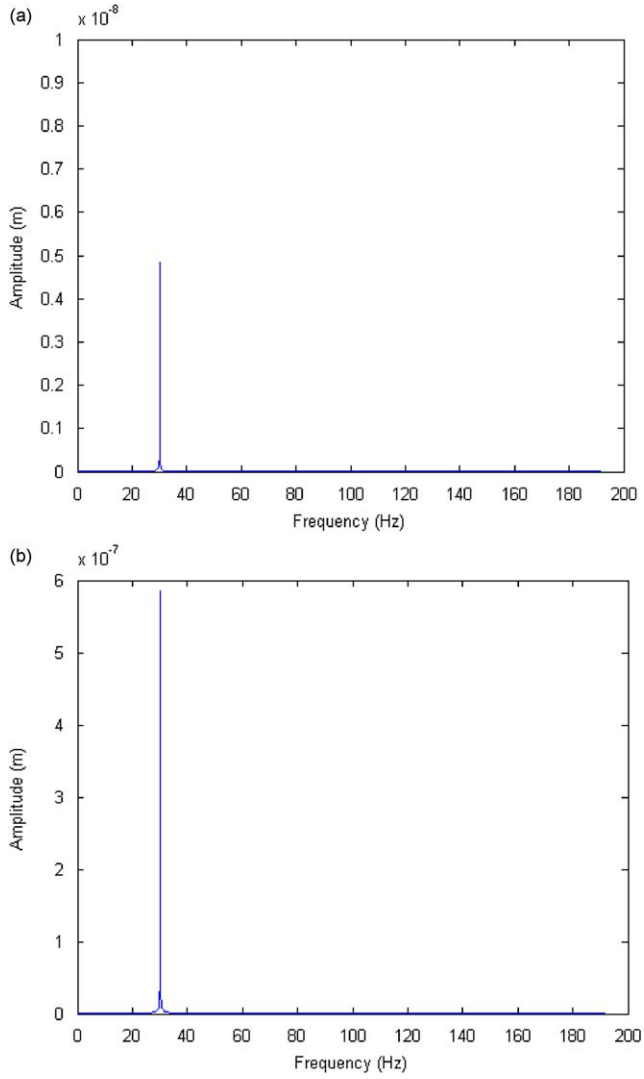

Fig. 6. Displacement spectra of a rotor–bearing system: (a) without unbalance and (b) with unbalance at bearing 1 location.

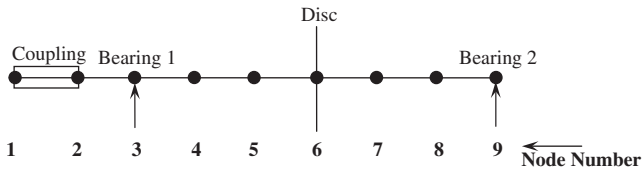

Fig. 7. FE model of rotor–coupling–bearing system showing node locations.

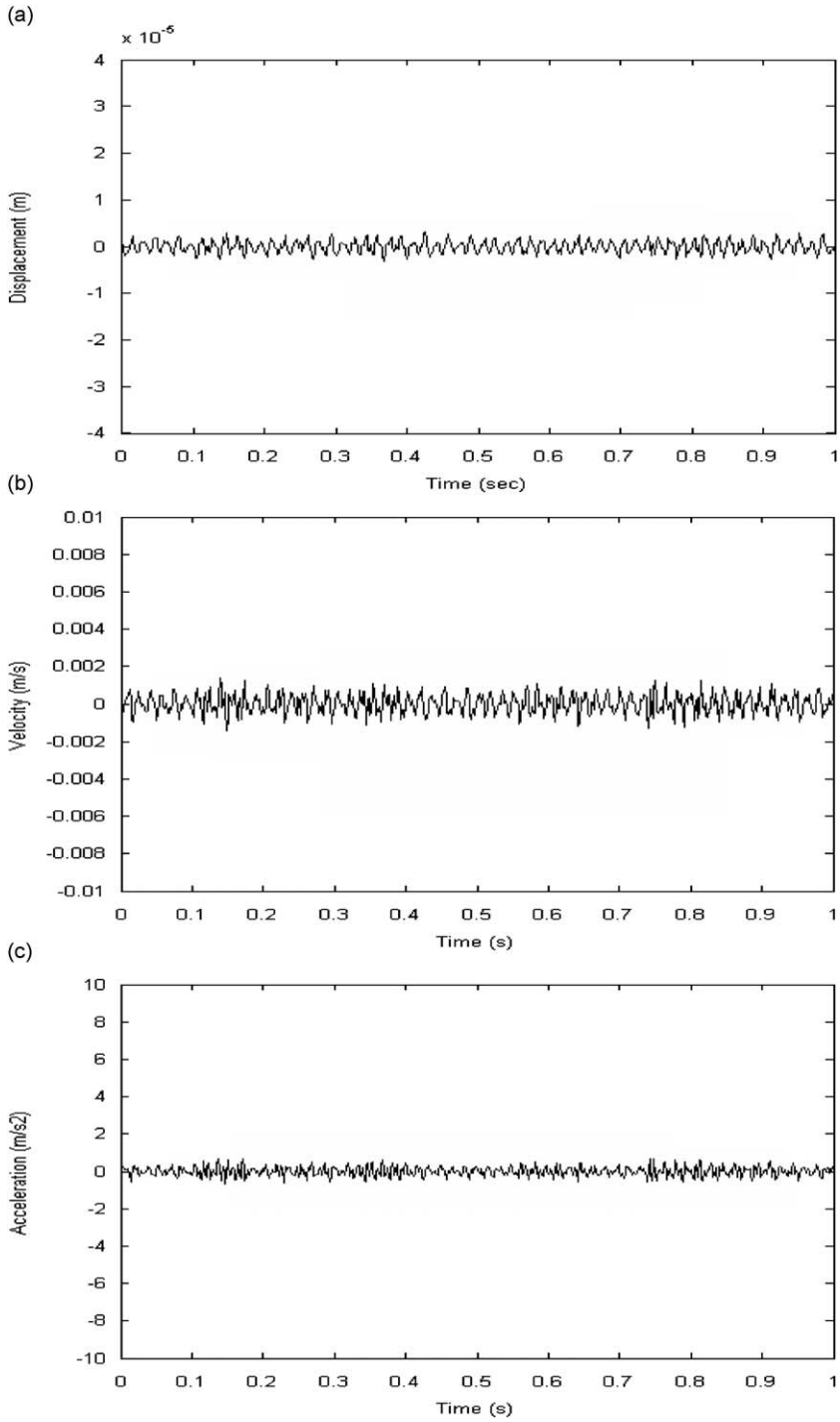

Fig. 8. Residual of: (a) displacement; (b) velocity and (c) acceleration for rotor system without misalignment at bearing 1 location in horizontal direction (*X*).

properties. The bearing stiffness and damping values are 3.8×10^7 N/m and 250 N s/m, respectively. The data of the rotor system are: power = 0.375 kW/50 Hz; torque = 1.04 N m; coupling: center of articulation = 29 mm; misalignment: parallel = 2 mm; angular = 0.5°. A steady-state analysis has been carried out for rotor–coupling–bearing system using finite element method for flexural vibration with parallel and angular misalignment of flexible couplings. The unbalance

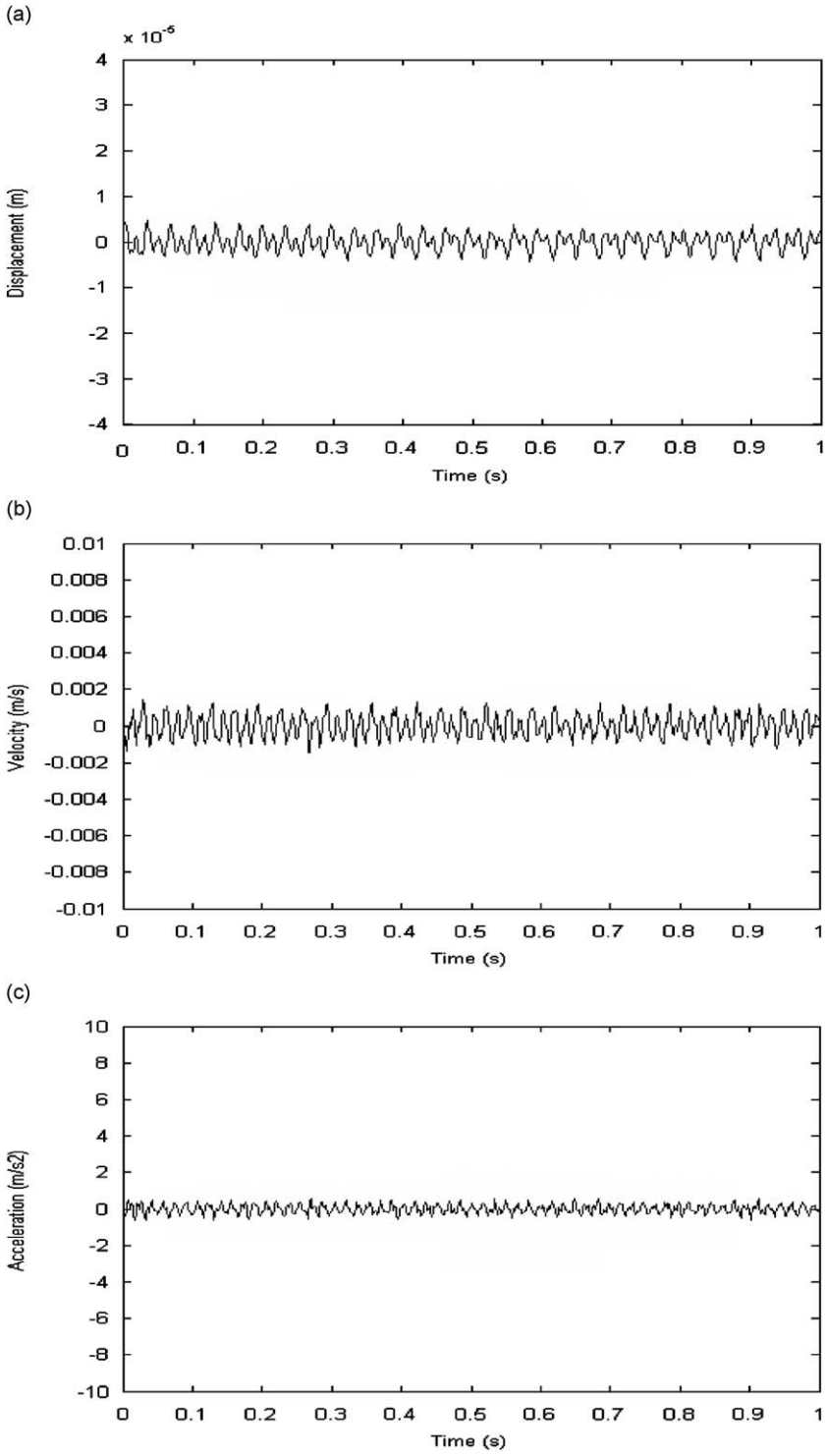

Fig. 9. Residual of: (a) displacement; (b) velocity and (c) acceleration for rotor system with 1 mm parallel misalignment at bearing 1 location in horizontal direction (*X*).

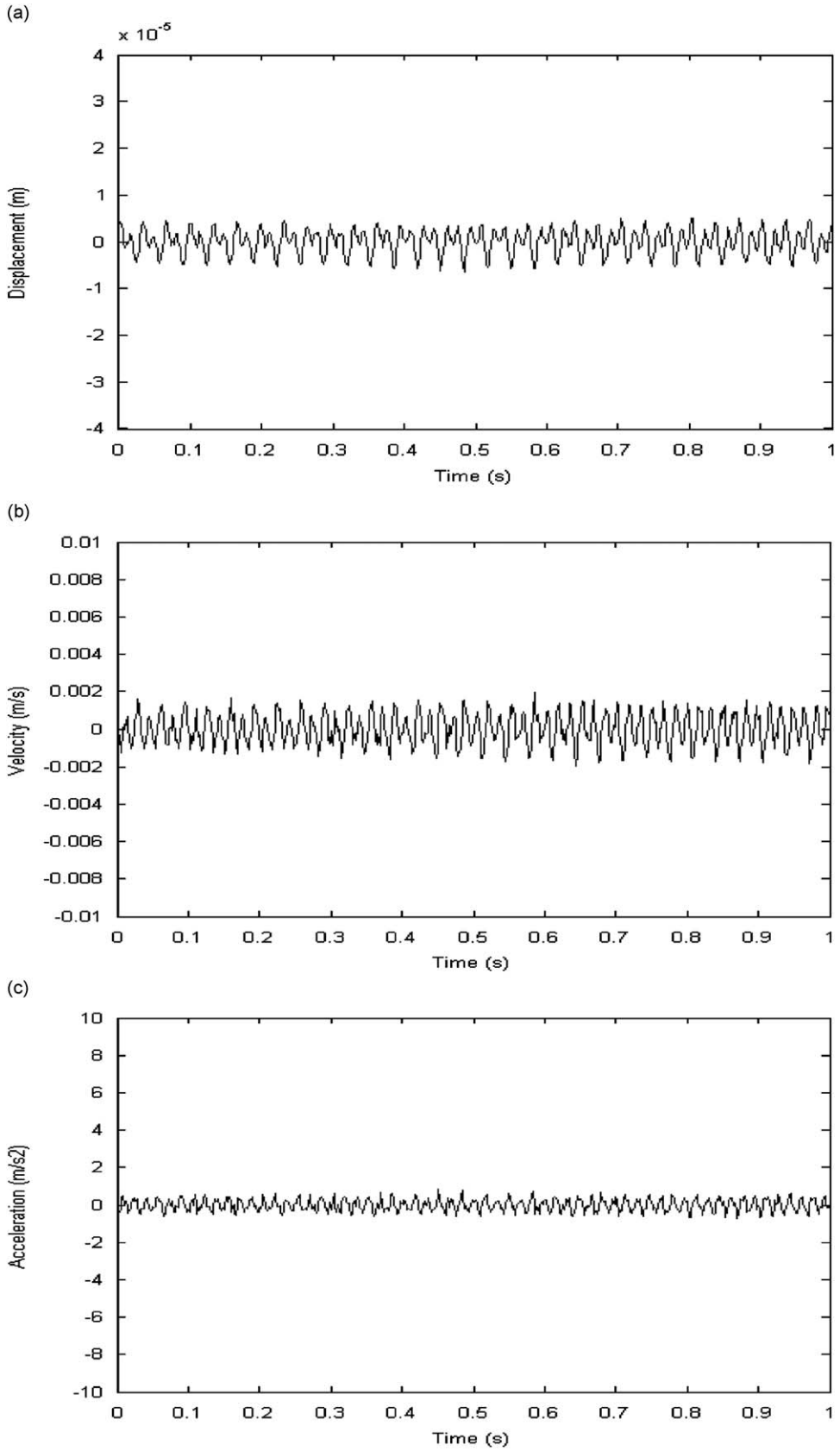

Fig. 10. Residual of: (a) displacement; (b) velocity and (c) acceleration for rotor system with 0.2° angular misalignment at bearing 1 location in horizontal direction (*X*).

force components in x and y directions can be written as

$$F_x = me\{\ddot{\theta}\sin\omega t + \dot{\theta}^2\cos\omega t\}, \quad F_y = me\{-\ddot{\theta}\cos\omega t + \dot{\theta}^2\sin\omega t\} \tag{18}$$

where m is the mass of unbalance, e the eccentricity, ω the angular speed and t the time.

The Houbolt time marching technique is used to model the system in time domain with a time step of 0.0015625 s. This analysis should be carried out at higher angular speed than critical speed and is chosen 30 Hz for this analysis. The displacement spectra of a rotor–coupling–bearing system without misalignment, with parallel misalignment and with angular misalignment at bearing 1 location are shown in Fig. 5.

Fig. 5 clearly shows the effect of misalignment. The frequency response of healthy rotor system shows $1\times$ running speed component only whereas for the rotor system with parallel misalignment and angular misalignment $1\times$ and $2\times$ running speed components are shown. This can be expected since coupling misalignment always affects $2\times$ running speed [2].

The steady-state analysis is also carried out for unbalance rotor system with different mass unbalance. The frequency domain responses obtained from steady-state analysis with unbalance and without unbalance are shown in Fig. 6.

The frequency response clearly shows increase in amplitude of $1\times$ running speed component only. This can be expected since the unbalance force rotates at the shaft running speed which affects the $1\times$ running speed only [2].

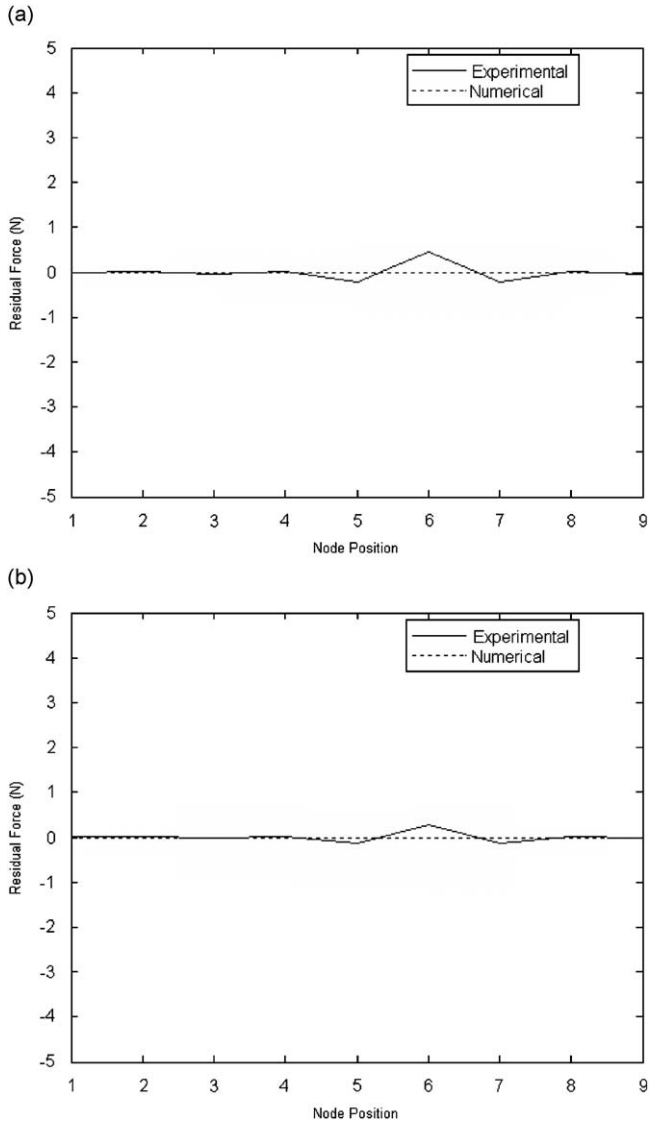

Fig. 11. Residual force at different locations along the rotor–bearing system without misalignment in: (a) horizontal and (b) vertical direction.

6. Experimental setup

The schematic diagram of experimental rotor–coupling–bearing system (Machinery Fault Simulator) is shown in Fig. 4. The shaft, 15.875 mm in diameter and 362 mm in length, is supported by two identical rolling element bearings ER 10K. A disk is mounted at the mid span of the shaft. The diameter of disk of mass 0.782 kg is 152.4 mm and thickness 15.875 mm. A tri-axial transducer Bruel & Kjaer 4321 has been used for data acquisition and analysis through OROS analyzer. The tri-axial transducer is placed on left side bearing (bearing 1) block to measure the acceleration amplitude in horizontal (*X*-axis) and vertical (*Y*-axis) directions. Measurement data are collected at rotor operating speed of 1800 rev/min (30 Hz). The data are stored and formulated through OROS analyzer to determine the velocity and displacement amplitudes by digital integration of measured acceleration data. Displacement data are transferred in MATLAB programming for further analysis.

7. Results

The analysis has been carried out using the finite element method for flexural vibrations at a steady speed of 1800 rev/min (30 Hz). For this analysis the parallel misalignment is varied from 0.0 to 2.0 mm, whereas angular misalignment is varied from 0° to 0.3°. To introduce unbalance in the system some standard masses are used in the disk at specific location.

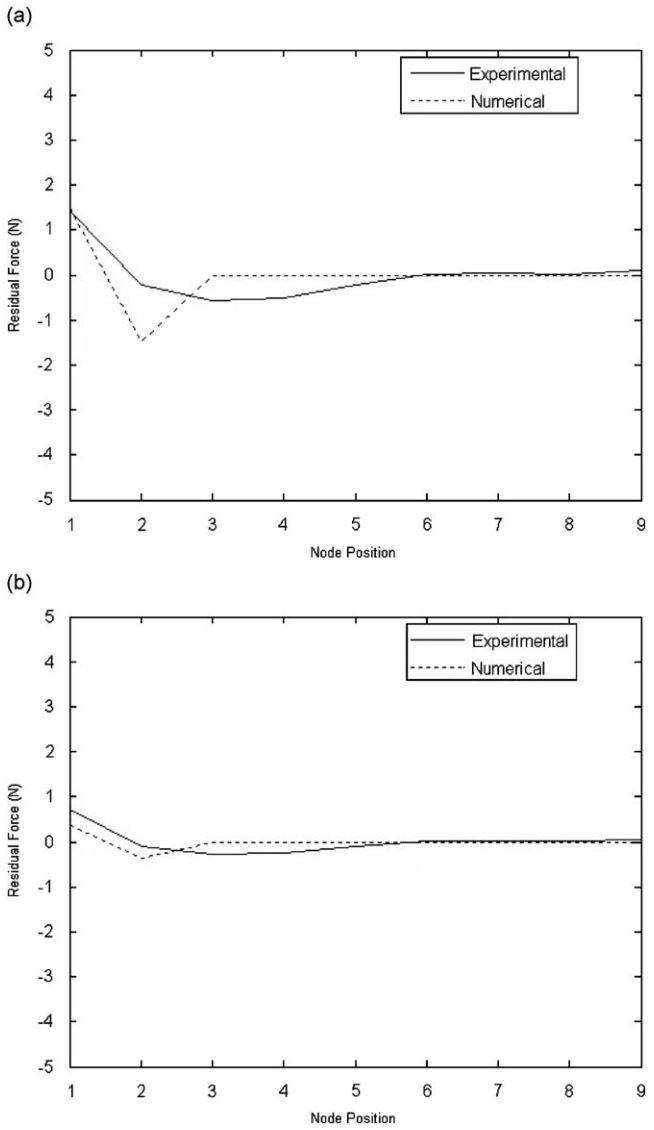

Fig. 12. Residual force at different locations along the rotor–bearing system with 1 mm parallel misalignment in: (a) horizontal and (b) vertical direction.

7.1. Coupling misalignment

In the present study, vibrations at all nine nodes i.e. 36 DOF of the model is considered. As only for few DOF the measured vibration data are available, for other DOF vibration data are estimated using modal expansion as discussed by Sekhar [11].

Vibration data for healthy (without misalignment and unbalance) as well as with parallel misalignment 1 mm in horizontal direction and angular misalignment 0.2° with horizontal axis is taken for this analysis. The residuals of displacement, velocity and acceleration at bearing 1 location in time domain for rotor system without misalignment, with parallel misalignment and with angular misalignment are shown in Figs. 8–10, respectively.

These residuals clearly show that the amplitudes of displacement, velocity and acceleration are increases due to effect of misalignment (for both parallel and angular). Now, to identify the fault, residual force (introduced due to misalignment) are calculated and compared with numerical model force. The residual forces, for both experimental and numerical, in horizontal and vertical direction for the system without misalignment, with parallel misalignment and with angular misalignment are shown in Figs. 11–13, respectively.

We consider the rotor–bearing system without misalignment to have no unbalance but in actual practice it is not possible to get zero unbalance system. As at node 6 (refer Fig. 7) the disk is mounted on the shaft some mass unbalance is always present at that node which is unavoidable. That is the reason behind a little residual force being created at node 6

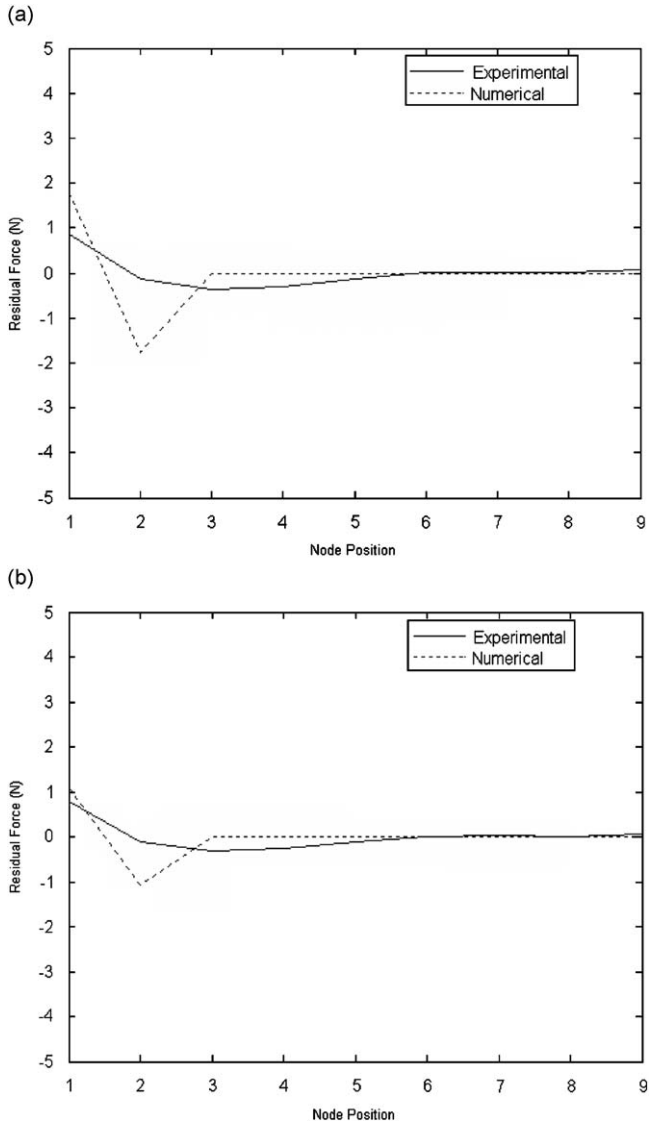

Fig. 13. Residual force at different locations along the rotor–bearing system with 0.2° angular misalignment in: (a) horizontal and (b) vertical direction.

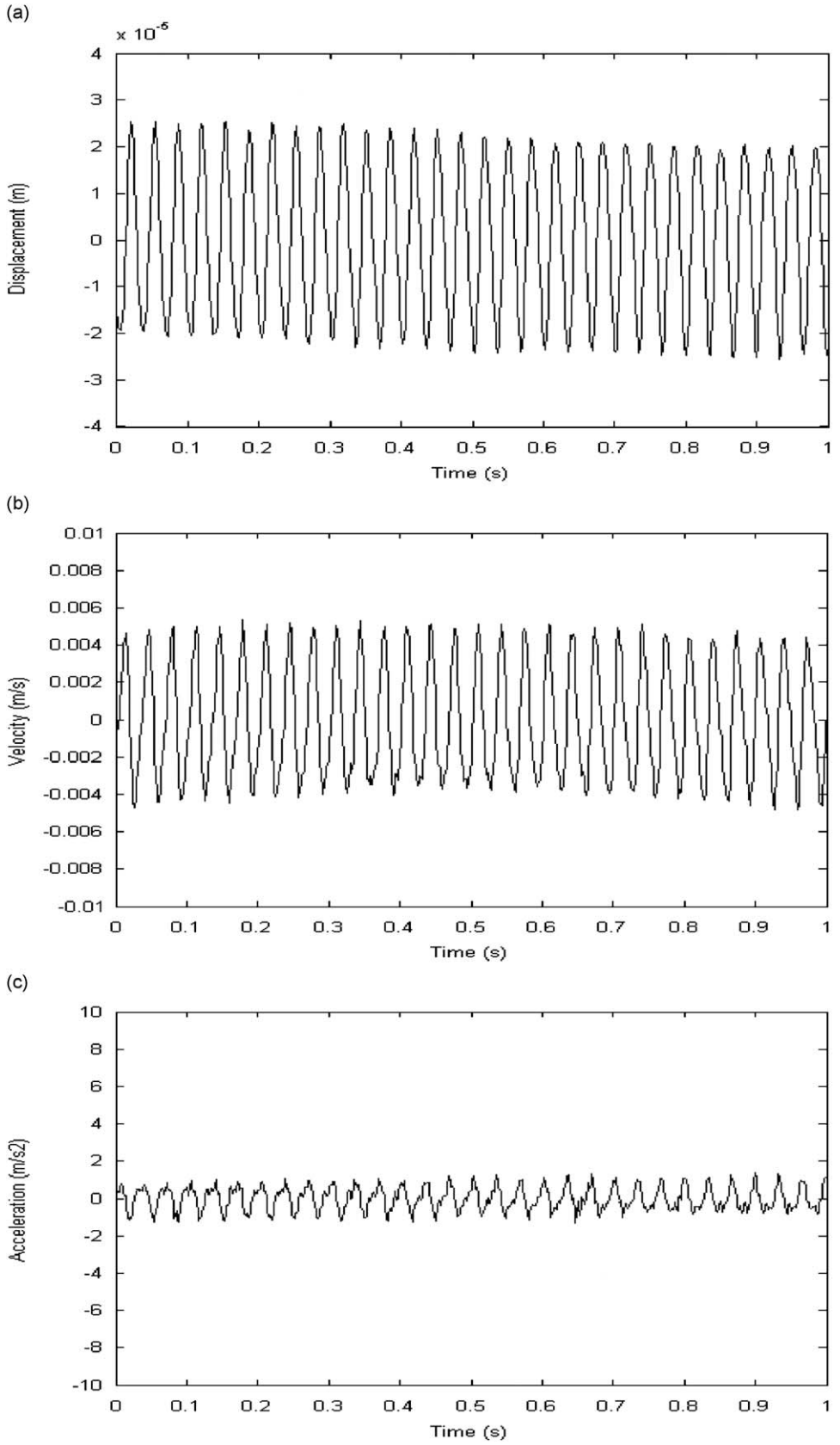

Fig. 14. Residual of: (a) displacement; (b) velocity and (c) acceleration for rotor system with unbalance at bearing 1 location in horizontal direction.

even for an intact system as shown in Fig. 11. Whereas Figs. 12 and 13 clearly show that the residual forces are observed only at nodes 1 and 2, which are the nodes of coupling (refer Fig. 7). Therefore, this method identifies the misalignment successfully.

7.2. Disk unbalance

Apart from the misalignment, fault due to disk unbalance has been simulated using the same technique. To introduce the unbalance in the system a mass of 6.14 g is attached to the disk at a location of 70 mm from the center. The residuals of displacement, velocity and acceleration at bearing 1 location with unbalance are shown in Fig. 14. Again in the same way

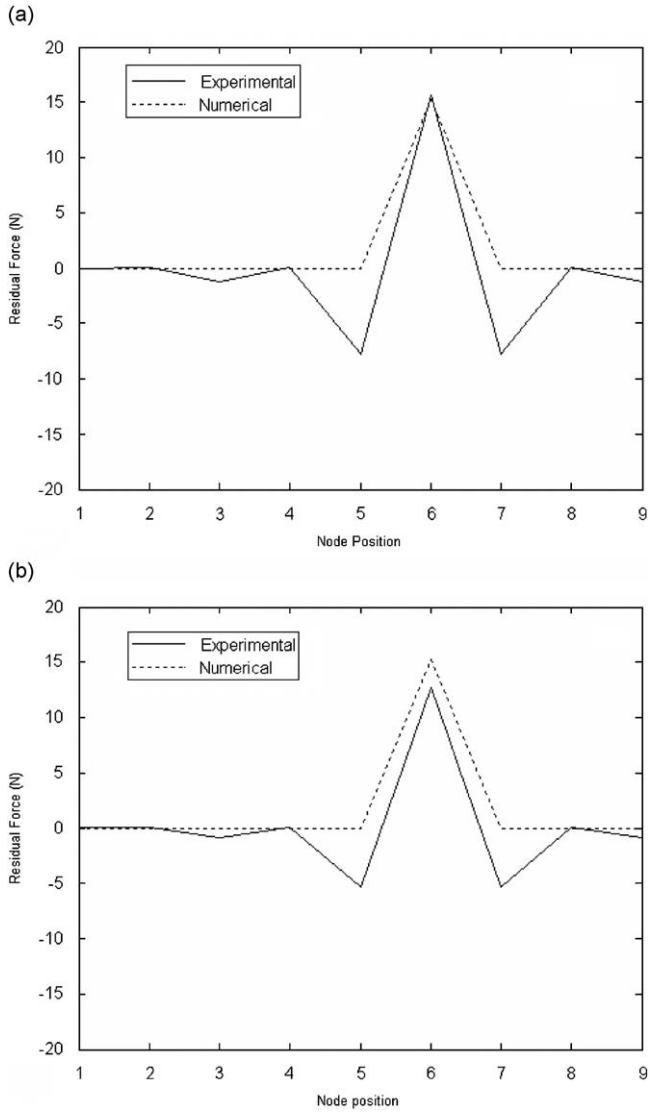

Fig. 15. Residual force at different locations along the rotor–bearing system in: (a) horizontal; (b) vertical direction for 4.298e−4 kg m unbalance on the disk.

Table 1
Comparison of predicted and actual unbalance.

Residual force at node 6 (N)	Predicted unbalance amount (g mm)	Actual unbalance amount (g mm)	Error (%)
22.63	636.916	694.280	8.262

the residual forces (introduced due to unbalance) are calculated and compared with numerical model force. The residual forces, for numerical and experimental studies, in horizontal and vertical direction due to unbalance are shown in Fig. 15.

These residuals in Figs. 8 and 14 clearly show that the amplitudes of displacement, velocity and acceleration are increases due to effect of unbalance. Fig. 15 clearly shows that the residual forces are observed at node 6, which is the node of disk unbalance. This figure also shows that this method identify the amount of unbalance. Therefore, this method identifies the disk unbalance successfully. Now to verify the predicted value of unbalance amount in the system, another amount of unbalance is introduced in the disk. The residual forces are calculated from the experimental results at same operating speed 30 Hz and predict the value of unbalance. The comparison of actual unbalance and predicted unbalance is presented in Table 1.

8. Conclusion

This method has thus demonstrated the model based fault detection system for a simple rotor–bearing system. This method may be useful for large systems like in turbine shafts, gearboxes and the like. Such a method has enormous potential in are automated diagnostics process where by the measurement of the responses, the fault condition and location can be detected. Then by simple measurement of the radial vibration alone and applying the proposed model based technique, faults of rotor–bearing system can easily be identified.

Appendix A

The rigid disk matrices:

$$[M_T^d]=\begin{bmatrix} M_d & 0 & 0 & 0\\ 0 & M_d & 0 & 0\\ 0 & 0 & 0 & 0\\ 0 & 0 & 0 & 0\end{bmatrix},\quad [M_R^d]=\begin{bmatrix} 0 & 0 & 0 & 0\\ 0 & 0 & 0 & 0\\ 0 & 0 & I_D & 0\\ 0 & 0 & 0 & I_D\end{bmatrix},\quad [G^d]=\begin{bmatrix} 0 & 0 & 0 & 0\\ 0 & 0 & 0 & 0\\ 0 & 0 & 0 & I_P\\ 0 & 0 & I_P & 0\end{bmatrix}$$

The finite shaft element matrices:

$$[M_T^e]=\frac{ml}{420}\begin{bmatrix} 156 & & & & & sym & & \\ 0 & 156 & & & & & & \\ 0 & -22l & 4l^2 & & & & & \\ 22l & 0 & 0 & 4l^2 & & & & \\ 54 & 0 & 0 & 13l & 156 & & & \\ 0 & 54 & -13l & 0 & 0 & 156 & & \\ 0 & 13l & -3l^2 & 0 & 0 & 22l & 4l^2 & \\ -13l & 0 & 0 & -3l^2 & -22l & 0 & 0 & 4l^2\end{bmatrix},\quad [M_R^e]=\frac{mr^2}{120l}\begin{bmatrix} 36 & & & & & sym & & \\ 0 & 36 & & & & & & \\ 0 & -3l & 4l^2 & & & & & \\ 3l & 0 & 0 & 4l^2 & & & & \\ -36 & 0 & 0 & -3l & 36 & & & \\ 0 & -36 & 3l & 0 & 0 & 36 & & \\ 0 & -3l & -l^2 & 0 & 0 & 3l & 4l^2 & \\ 3l & 0 & 0 & -l^2 & -3l & 0 & 0 & 4l^2\end{bmatrix}$$

$$[G^e]=\frac{2mr^2}{120l}\begin{bmatrix} 0 & & & & skew & sym & & \\ 36 & 0 & & & & & & \\ -3l & 0 & 0 & & & & & \\ 0 & -3l & 4l^2 & 0 & & & & \\ 0 & 36 & -3l & 0 & 0 & & & \\ -36 & 0 & 0 & -3l & 36 & 0 & & \\ -3l & 0 & 0 & l^2 & 3l & 0 & 0 & \\ 0 & -3l & -l^2 & 0 & 0 & 3l & 4l^2 & 0\end{bmatrix},\quad [K_B^e]=\frac{EI}{l^3}\begin{bmatrix} 12 & & & & & & sym & \\ 0 & 12 & & & & & & \\ 0 & -6l & 4l^2 & & & & & \\ 6l & 0 & 0 & 4l^2 & & & & \\ -12 & 0 & 0 & -6l & 12 & & & \\ 0 & -12 & 6l & 0 & 0 & 12 & & \\ 0 & -6l & -2l^2 & 0 & 0 & 6l & 4l^2 & \\ 6l & 0 & 0 & 2l^2 & -6l & 0 & 0 & 4l^2\end{bmatrix}$$

$$[K_A^e]=\frac{P}{30l}\begin{bmatrix} 36 & & & & & sym & & \\ 0 & 36 & & & & & & \\ 0 & -3l & 4l^2 & & & & & \\ 3l & 0 & 0 & 4l^2 & & & & \\ -36 & 0 & 0 & -3l & 36 & & & \\ 0 & -36 & 3l & 0 & 0 & 36 & & \\ 0 & -3l & -l^2 & 0 & 0 & 3l & 4l^2 & \\ 3l & 0 & 0 & -l^2 & -3l & 0 & 0 & 4l^2\end{bmatrix}$$

Coupling stiffness matrix:

$$[K] = \frac{EI}{l^3}\begin{bmatrix} 12 & & & & & sym & & \\ 0 & 12 & & & & & & \\ 0 & -6l & 4l^2 & & & & & \\ 6l & 0 & 0 & 4l^2 & & & & \\ -12 & 0 & 0 & -6l & 12 & & & \\ 0 & -12 & 6l & 0 & 0 & 12 & & \\ 0 & -6l & -2l^2 & 0 & 0 & 6l & 4l^2 & \\ 6l & 0 & 0 & 2l^2 & -6l & 0 & 0 & 4l^2 \end{bmatrix}$$

References

[1] E. Kramer, *Dynamics of Rotors and Foundations*, Springer, Berlin, 1993.
[2] M. Xu, R.D. Marangoni, Vibration analysis of a motor-flexible coupling-rotor system subject to misalignment and unbalance—part 1: theoretical model and analysis, *Journal of Sound and Vibration* 176 (5) (1994) 663–679.
[3] C.B. Gibbons, Coupling misalignment forces, *Proceedings of the Fifth Turbomachinery Symposium*, Gas Turbine Laboratories, Texas, 1976, pp. 1111–1116.
[4] A.S. Sekhar, B.S. Prabhu, Effects of coupling misalignment on vibrations of rotating machinery, *Journal of Sound and Vibration* 185 (4) (1995) 655–671.
[5] S. Prabhakar, A.S. Sekhar, A.R. Mohanty, Crack versus coupling misalignment in a transient rotor system, *Journal of Sound and Vibration* 256 (4) (2002) 773–786.
[6] V. Vowk, *Machinery Vibration*, McGraw-Hill, New York, 1991.
[7] J. Piotrowski, *Shaft Alignment Handbook*, Marcel Dekker, New York, 1986.
[8] R. Platz, R. Markert, Fault models for on-line identification of malfunctions in rotor system, *Transaction of Fourth International Conference on Acoustical and Vibratory Surveillance*, France, 2001, pp. 435–446.
[9] H.D. Nelson, J.M. McVaugh, The dynamics of rotor–bearing system using finite elements, *American Society of Mechanical Engineers Journal of Engineering for Industry* 98 (2) (1976) 593–600.
[10] R. Isermann, Fault diagnosis of machines via parameter estimation and knowledge processing, *Automatica* 29 (4) (1993) 815–835.
[11] A.S. Sekhar, Crack identification in a rotor system: a model based approach, *Journal of Sound and Vibration* 270 (2004) 887–902.
[12] A.S. Sekhar, Multiple cracks effects and identification, *Mechanical Systems and Signal Processing* 22 (2008) 845–878.
[13] E.Y. Chow, A.S. Willsky, Analytical redundancy and the design of robust detection systems, *IEEE Transactions on Automatic Control* 29 (7) (1984) 603–614.
[14] J. Gertler, Residual generation in model based fault diagnosis, *Control Theory and Advanced Technology* 9 (1) (1993) 259–285.
[15] P.M. Frank, L. Keller, Sensitivity discriminating observer design for instrument failure detection, *IEEE Transactions on Aerospace Electron System* AES-16 (1980) 460–467.
[16] R. Isermann, Model based fault detection and diagnosis methods, *Proceedings of the American Control Conference*, Seattle, WA, USA, June 1995, pp. 1605–1609.
[17] R.J. Patton, P.M. Frank, R.N. Clark (Eds.). Fault Diagnosis in Dynamic Systems, Theory and Application, Control Engineering Series, Prentice-Hall, London, 1989.
[18] R. Merkert, R. Platz, M. Seidler, Model based fault identification in rotor systems by least square fitting, *International Journal of Rotating Machinery* 7 (5) (2001) 311–321.